

See discussions, stats, and author profiles for this publication at: <https://www.researchgate.net/publication/263939700>

# In-Situ Synthesis of Multicompartment Nanoparticles of Linear BAC Triblock Terpolymer by Seeded RAFT Polymerization

ARTICLE in MACROMOLECULES · MARCH 2014

Impact Factor: 5.8 · DOI: 10.1021/ma5002386

---

CITATIONS

12

READS

23

## 5 AUTHORS, INCLUDING:



Shentong Li

Nankai University

17 PUBLICATIONS 166 CITATIONS

[SEE PROFILE](#)



Quanlong Li

Nankai University

14 PUBLICATIONS 117 CITATIONS

[SEE PROFILE](#)



Qu Yaqing

Nankai University

5 PUBLICATIONS 15 CITATIONS

[SEE PROFILE](#)



Wangqing Zhang

Nankai University

105 PUBLICATIONS 2,221 CITATIONS

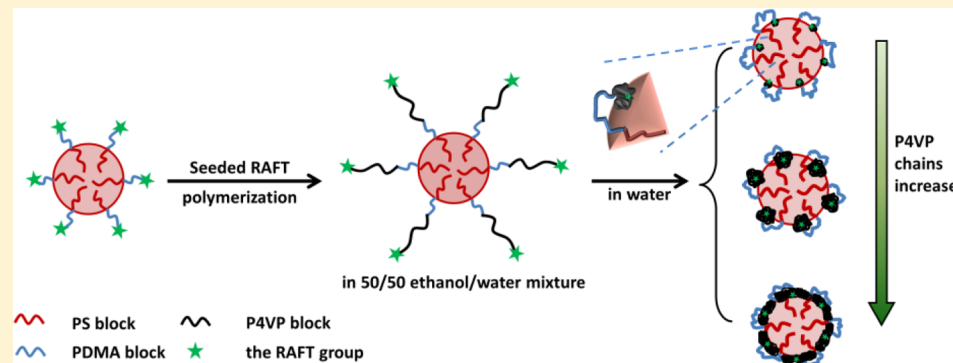
[SEE PROFILE](#)

## In-Situ Synthesis of Multicompartment Nanoparticles of Linear BAC Triblock Terpolymer by Seeded RAFT Polymerization

Fei Huo, Shentong Li, Quanlong Li, Yaqing Qu, and Wangqing Zhang\*

Key Laboratory of Functional Polymer Materials of the Ministry of Education, Collaborative Innovation Center of Chemical Science and Engineering (Tianjin), Institute of Polymer Chemistry, Nankai University, Tianjin 300071, China

Supporting Information



**ABSTRACT:** A new strategy of in-situ synthesis of multicompartment nanoparticles of the linear BAC triblock terpolymer of polystyrene-*b*-poly(*N,N*-dimethylacrylamide)-*b*-poly(4-vinylpyridine) (PS-*b*-PDMA-*b*-P4VP) is proposed. This strategy includes the initial seeded RAFT polymerization of 4-vinylpyridine in the ethanol/water mixture (50/50 by weight), which is the solvent for the C block of the newly formed poly(4-vinylpyridine) (P4VP), in the presence of the diblock copolymer seed nanoparticles of polystyrene-*b*-poly(*N,N*-dimethylacrylamide) trithiocarbonate with the Z-group RAFT terminal at the outer side of the solvophilic A block of poly(*N,N*-dimethylacrylamide) (PDMA), and the subsequent transfer of the in-situ synthesized core-corona nanoparticles of PS-*b*-PDMA-*b*-P4VP containing a polystyrene (PS) core and a diblock corona of poly(*N,N*-dimethylacrylamide)-*b*-poly(4-vinylpyridine) into water to deposit the C block of the newly formed P4VP block onto the PS core to form discrete P4VP nodules to form multicompartment nanoparticles. With the increasing polymerization degree of the P4VP block, the multicompartment nanoparticles can convert into concentric core–shell–corona nanoparticles. Two reasons of (1) the P4VP block being immiscible with the PS block and (2) the special seeded RAFT polymerization avoiding the P4VP block being entrapped into the PS core are ascribed to the successful preparation of the linear BAC triblock terpolymer multicompartment nanoparticles.

### 1. INTRODUCTION

Over the past decade, multicompartment micelles (MCMs) have aroused great interest since it was first proposed by Ringsdorf in the late 1990s.<sup>1–5</sup> This multicompartment structure mimics somewhat the complex organization of eukaryotic cells and has the potential of the simultaneous storage or release of different stored chemicals.<sup>6</sup> Compared with the general polymeric micelles which usually consist of a single solvophobic core domain, MCMs are designed as more elaborate structure with discrete domains of two solvophobic fragments that are mutually incompatible and a surrounding corona of a solvophilic fragment that stabilizes the solvophobic domains. From this consideration, there are generally four strategies to synthesize these MCMs: (1) Micellization of linear ABC or BAC triblock terpolymers<sup>7–22</sup> or linear ABCA and ABCBA multiblock polymers<sup>23–27</sup> (A represents the solvophilic block, and B and C represent the two incompatible solvophobic blocks throughout this article). In the selective solvent for the A

block (A-selective solvent), the two incompatible solvophobic B and C blocks form the phase-separated core and the solvophilic A block forms the corona, and raspberry-like or soccer-ball-like MCMs can be formed.<sup>9,10,17</sup> (2) Micellization of ABC miktoarm star terpolymers,<sup>28–34</sup> in which the three blocks mandatorily converge at a common point and thereby constrain the resulting A, B, and C nanodomains to meet along a common curve, and this in turn leads to segregation of all three mutually immiscible polymer chains at their jointed point to form well-defined MCMs. (3) Comicellization of AB and BC diblock copolymers in the A-selective solvent.<sup>35–39</sup> This strategy has the advantages of the convenient synthesis of diblock copolymer compared with the ABC or BAC triblock terpolymers and the tunable structure of MCMs by changing

Received: January 31, 2014

Revised: March 3, 2014

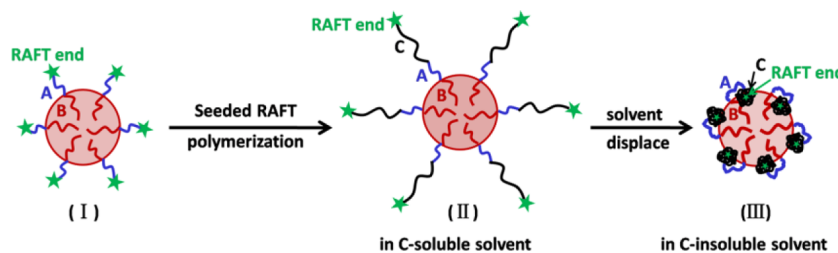
Published: March 17, 2014



ACS Publications

© 2014 American Chemical Society

**Scheme 1. In-Situ Synthesis of the Multicompartment Nanoparticles of Linear BAC Triblock Terpolymer by Seeded RAFT Polymerization**



the ratio of the AB and BC diblock copolymers.<sup>(4)</sup> Micellization of (A-graft-B)-block-(A-graft-C) block terpolymers, in which the two incompatible side chains of B and C form two phase-separated core domains.<sup>40–42</sup> Of all the four strategies mentioned above,<sup>7–42</sup> the micellization of linear ABC or BAC triblock terpolymers to prepare MCMs may be the most popular. However, this strategy suffers from three disadvantages. First, the phase separation of the B and C blocks in the core layer is the key to prepare well-defined MCMs, and therefore fluorinated ABC or BAC linear triblock terpolymers are usually needed,<sup>9–16</sup> although some cases of nonfluorinated triblock terpolymers have been reported.<sup>17–22</sup> Synthesis of fluorinated triblock terpolymers is generally a laborious work and therefore limits its extensive application. Second, linear ABC or BAC triblock terpolymers have the tendency to form concentric core–shell–corona micelles instead of multicompartment nanostructures with two phase-separated core domains.<sup>43–47</sup> Note: concentric core–shell–corona micelles do not satisfy a strict definition of MCMs, since each compartment does not have independent access to the exterior of the micelles and thus fails to ensure the independent chemical function of different components. Third, the strategy as well as the other three ones as introduced above usually affords very diluted MCMs dispersion (usually below 1 wt %) to ensure the colloidal stability and also suffers from the drawback of the time-consuming and/or multiple steps.<sup>9–42</sup> Thus, convenient synthesis of concentrated and nonfluorinated MCMs of linear ABC or BAC triblock terpolymers is a challenge in polymer chemistry and physics.

Seeded polymerization is a convenient method to synthesize polymeric nanoparticles.<sup>48–51</sup> By employing the reversible addition–fragmentation chain transfer (RAFT) polymerization technology in seeded polymerization, block copolymer nano-objects with much higher polymer concentration than those of block copolymer micelles can be prepared.<sup>52–58</sup> For example, An and co-workers prepared block copolymer nanoparticle clusters and linear/branched fibers by seeded emulsion RAFT polymerization of styrene employing the core cross-linked star polymers as macro-RAFT agent.<sup>52</sup> Recently, we have proposed a seeded dispersion RAFT polymerization to afford BAB triblock copolymer flower-like nanoparticles.<sup>58</sup> In this seeded dispersion RAFT polymerization, the core–corona nanoparticles of polystyrene-*b*-poly(*N,N*-dimethylacrylamide) (PS-*b*-PDMA) containing a PS core and a PDMA corona with the Z-group RAFT terminal (note: Z-group is the activating group and R-group is the reinitiating group in the RAFT agent as defined in ref 59) on the outside of the PDMA block were used as seed nanoparticles. During the seeded dispersion RAFT polymerization, the newly formed PS block deposited on the PS core of the seed nanoparticles to prepare well-defined

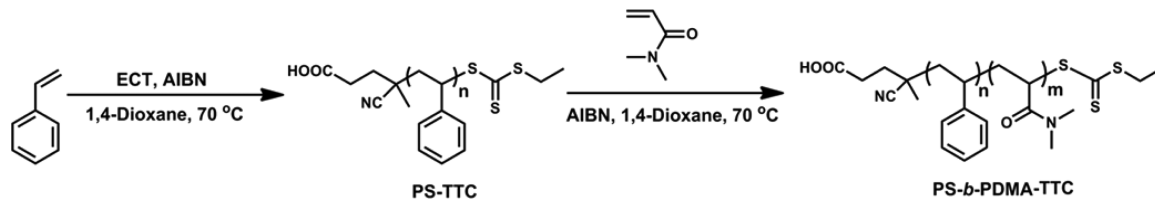
flower-like BAB triblock copolymer nanoparticles with the looped PDMA block as corona.

Inspired by these successes,<sup>52–58</sup> a new strategy named seeded RAFT polymerization herein as shown in Scheme 1 is proposed to synthesize multicompartment nanoparticles of linear BAC triblock terpolymer. This strategy includes (1) the preparation of the diblock copolymer seed nanoparticles of PS-*b*-PDMA containing a PS core of the B block and a PDMA corona of the A block with the Z-group RAFT terminal on the outside of the A block, (2) RAFT polymerization of 4-vinylpyridine to introduce the C block of poly(4-vinylpyridine) (P4VP) to prepare BAC triblock terpolymer core–corona nanoparticles of polystyrene-*b*-poly(*N,N*-dimethylacrylamide)-*b*-poly(4-vinylpyridine) (PS-*b*-PDMA-*b*-P4VP) containing a PS core and a diblock corona of PDMA-*b*-P4VP in the C-selective solvent, and (3) the transfer of the in-situ synthesized BAC triblock terpolymer core–corona nanoparticles into the non-solvent for the C block of P4VP to deposit the P4VP chains as discrete P4VP nodules on the PS core to form multicompartment nanoparticles. It has been demonstrated that linear BAC triblock terpolymer nano-objects ranging from multicompartment nanoparticles to concentric core–shell–corona nanoparticles dependent on the polymerization degree of the newly formed C block of P4VP can be prepared through this in-situ synthesis strategy. The synthesis of the well-defined multicompartment nanoparticles is ascribed to the seeded RAFT polymerization, which is performed in the C-selective solvent much different from the previous seeded dispersion RAFT polymerization,<sup>58</sup> since it avoids the newly formed P4VP block being entrapped in the PS core to lead to two well-phase-separated core domains.

## 2. EXPERIMENTAL SECTION

**2.1. Materials.** The monomers of *N,N*-dimethylacrylamide (DMA, 99.5%, Alfa), 4-vinylpyridine (4VP, 96%, Alfa), and styrene (St, >98%, Tianjin Chemical Company) were distilled under reduced pressure prior to use. The RAFT agent of 4-cyan-4-(ethylsulfanylthiocarbonyl)sulfanylpentanoic acid (ECT) was synthesized as discussed elsewhere.<sup>60</sup> The initiator of 2,2'-azobis(2-methylpropionitrile) (AIBN, >99%, Tianjin Chemical Company) was purified by recrystallization from ethanol. The internal standard of 1,3,5-trioxane (98%, Alfa) for the <sup>1</sup>H NMR analysis and other reagents were analytic grade and were used as received.

**2.2. Synthesis of the PS-*b*-PDMA-TTC Diblock Copolymer.** The diblock copolymer of polystyrene-*b*-poly(*N,N*-dimethylacrylamide) trithiocarbonate (PS-*b*-PDMA-TTC, in which TTC represents the RAFT terminal of trithiocarbonate) was synthesized by sequential RAFT polymerization. Into a 50 mL Schlenk flask with a magnetic bar, St (16.00 g, 0.154 mol), ECT (101.0 mg, 0.384 mmol), and AIBN (21.0 mg, 0.128 mmol) dissolved in 1,4-dioxane (8.00 g) were added. The solution was initially degassed with nitrogen at 0 °C for 30 min, and then the flask content was immersed into a preheated oil bath at 70 °C for 22 h. The polymerization was quenched at 50.3% monomer

**Scheme 2.** Synthesis of the PS-*b*-PDMA-TTC Diblock Copolymer

conversion at 22 h by rapid cooling upon immersion of the flask in iced water, in which the monomer conversion was determined by  $^1\text{H}$  NMR analysis in the presence of the internal standard of 1,3,5-trioxane. The synthesized polymer was precipitated into ethanol, collected by three precipitation/filtration cycles, and then dried at room temperature under vacuum to afford the PS-TTC macro-RAFT agent.

Into a 25 mL Schlenk flask with a magnetic bar, the synthesized PS-TTC (7.92 g, 0.404 mmol), DMA (4.00 g, 40.4 mmol), and AIBN (22.1 mg, 0.135 mmol) dissolved in 1,4-dioxane (6.0 g) were added. The oxygen dissolved in the solution was removed by nitrogen purging, and then the polymerization was performed at 70 °C. After 2 h polymerization with the monomer conversion at 79.8%, which was determined by  $^1\text{H}$  NMR analysis in the presence of the internal standard of 1,3,5-trioxane, the polymerization was quenched by rapid cooling upon immersion of the flask into iced water. The synthesized polymer was precipitated into the mixture of diethyl ether and *n*-hexane (3:1 by weight), collected by three precipitation/filtration cycles, washed twice with ethanol, and last dried at room temperature under vacuum to afford the PS-*b*-PDMA-TTC diblock copolymer.

### 2.3. Preparation of the PS-*b*-PDMA-TTC Seed Nanoparticles.

Into a 25 mL Schlenk flask with a magnetic bar, the synthesized PS-*b*-PDMA-TTC diblock copolymer (0.693 g, 0.024 mmol) and the ethanol/water mixture (6.00 g, 50/50 by weight), which is named as the 50/50 ethanol/water mixture in the subsequent discussion, were added, and then the mixture was dispersed by means of an ultrasonic bath for 30 min (KQ-200 KDE, 40 kHz, 200 W, Zhoushan, China). Subsequently, the monomer of 4VP (1.00 g, 9.52 mmol) was added, and the vigorous stirring for 30 min was followed to afford an opalesque dispersion of the PS-*b*-PDMA-TTC seed nanoparticles. To avoid any unwanted side effect, the freshly prepared dispersion of the PS-*b*-PDMA-TTC seed nanoparticles was used in the subsequent seeded RAFT polymerization.

**2.4. Seeded RAFT Polymerization and Synthesis of the Multicompartment Nanoparticles.** The seeded RAFT polymerization of 4VP in the 50/50 ethanol/water mixture at 70 °C was performed with the molar ratio of  $[4\text{VP}]_0:[\text{PS-}b\text{-PDMA-TTC}]_0:[\text{AIBN}]_0 = 1200:3:1$  and with the weight percent of the fed monomer plus the PS-*b*-PDMA-TTC seed nanoparticles at 15%. Typically, into the freshly prepared dispersion of the PS-*b*-PDMA-TTC seed-nanoparticles (0.693 g, 0.024 mmol) containing a given weight of the 4VP monomer (1.00 g, 9.52 mmol) and the 50/50 ethanol/water mixture (6.00 g), the initiator of AIBN (1.30 mg, 0.0079 mmol) dissolved in the 50/50 ethanol/water mixture (3.60 g) was added. The flask content was vigorously stirred for 10 min, degassed with nitrogen at 0 °C for 30 min, and then the polymerization was initiated by immersing the flask into preheated oil bath at 70 °C. After a given time, the polymerization was quenched by immersing the flask in iced water.

$$\text{conversion (\%)} = \frac{I_{8.05-8.57} - 3I_{5.45-5.55}}{I_{8.05-8.57}} \times 100\% \quad (1)$$

The monomer conversion in the seeded RAFT polymerization was detected by  $^1\text{H}$  NMR analysis, in which a drop of the polymerization solution (about 0.1 mL) was diluted with  $\text{DMSO}-d_6$  (0.5 mL) and subjected to  $^1\text{H}$  NMR analysis to determine the monomer conversion following eq 1, in which  $I_{5.45-5.55}$  is the integral area of the vinyl signals at  $\delta = 5.45-5.55$  ppm in the remaining monomer and  $I_{8.05-8.57}$  is the integral area of the pyridyl signals at  $\delta = 8.05-8.57$  corresponding to

both the 4VP monomer and the P4VP block in the synthesized polymer.

To detect the morphology of the PS-*b*-PDMA-*b*-P4VP triblock terpolymer nano-objects, part of the in-situ synthesized PS-*b*-PDMA-*b*-P4VP triblock terpolymer nano-objects dispersed in the polymerization medium of the 50/50 ethanol/water mixture was bubbled with  $\text{N}_2$  to remove ethanol. During the  $\text{N}_2$  bubbling, a suitable amount of water was added to keep no obvious change in the triblock terpolymer concentration. Then, the colloidal dispersion was diluted with suitable water, and a small drop of the diluted dispersion was deposited onto a piece of copper grid covered with thin film of carbon, dried at room temperature, stained in  $\text{I}_2$  vapor at 50 °C for 60 min under reduced pressure, and last observed by a transmission electron microscope (TEM).

To collect the PS-*b*-PDMA-*b*-P4VP triblock terpolymer for the gel permeation chromatography (GPC) analysis,  $^1\text{H}$  NMR analysis, and the differential scanning calorimetry (DSC) analysis, part of the polymerization dispersion of the PS-*b*-PDMA-*b*-P4VP triblock terpolymer nano-objects was precipitated into the mixture of acetone and *n*-hexane (1:1), washed twice with *n*-hexane, and finally dried at room temperature under vacuum to afford the triblock terpolymer in pale yellow.

**2.5. Characterization.** The  $^1\text{H}$  NMR analysis was performed on a Bruker Avance III 400 MHz NMR spectrometer using  $\text{CDCl}_3$  or  $\text{DMSO}-d_6$  as solvent. To obtain the molecular weight and its distribution or the polydispersity index (PDI,  $\text{PDI} = M_w/M_n$ ) of the synthesized polymers, the GPC analysis was detected using a Viscotek GPC Max Ve2001 solvent/sample module equipped with a DAWN HELEOS 8 light scattering photometer, a ViscoStar viscometer, and an Optilab rEX interferometric refractometer from Wyatt Technology Corporation. Samples were passed through three Mz-Gel SD plus 10  $\mu\text{m}$  columns using DMF as eluent at flow rate of 1.0 mL/min at 25 °C with narrowly polydispersed polystyrene as calibration standard. Dynamic light scattering (DLS) analysis was performed on a Nano-ZS90 (Malvern) laser light scattering spectrometer with He-Ne laser at the wavelength of 633 nm at 90° angle, in which the hydrodynamic diameter  $D_h$  was determined by intensity following the CONTIN method. TEM observation was performed using a Tecnai G<sup>2</sup> F20 electron microscope at an acceleration of 200 kV. DSC analysis was carried out on a NETZSCH differential scanning calorimeter under a nitrogen atmosphere, in which the sample was heated to 200 °C at the heating rate of 10 °C/min, cooled to -20 °C in 5 min, and then heated to 200 °C at the heating rate of 10 °C/min.

## 3. RESULTS AND DISCUSSION

**3.1. Synthesis of the PS-*b*-PDMA-TTC Diblock Copolymer.** The PS-*b*-PDMA diblock copolymer was prepared by sequential RAFT polymerization as shown in Scheme 2,<sup>58</sup> in which the initial synthesis of the macromolecular RAFT (macro-RAFT) agent of PS-TTC and the subsequent PS-TTC mediated polymerization of DMA are included.

The PS-TTC macro-RAFT agent was synthesized via RAFT polymerization of St in 1,4-dioxane using ECT as RAFT agent and AIBN as initiator under  $[\text{St}]_0:[\text{ECT}]_0:[\text{AIBN}]_0 = 1200:3:1$ . The RAFT polymerization of styrene was quenched at 50.3% monomer conversion to ensure the narrowly dispersed molecular weight of the synthesized PS-TTC. The theoretical number-average molecular weight ( $M_{n,\text{th}}$ ) of PS-TTC is 21.2

kg/mol, corresponding to the polymerization degree (DP) at 201, in which  $M_{n,\text{th}}$  is calculated following eq 2. The DMF-based GPC analysis gives the polymer molecular weight  $M_{n,\text{GPC}} = 20.6 \text{ kg/mol}$ , which is very close to  $M_{n,\text{th}}$  and the PDI value is as narrow as 1.07 (Figure 1). The  $^1\text{H}$  NMR spectrum of PS-

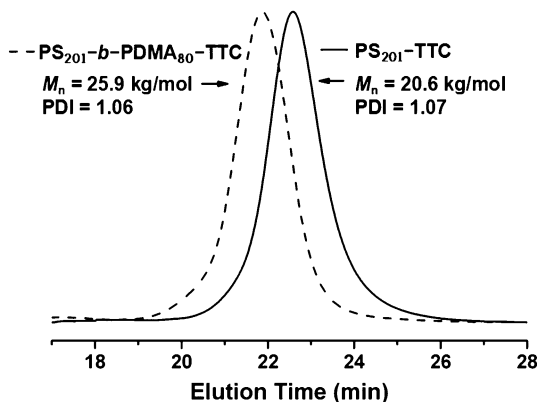


Figure 1. GPC traces of the PS<sub>201</sub>-TTC homopolymer and the PS<sub>201</sub>-b-PDMA<sub>80</sub>-TTC diblock copolymer.

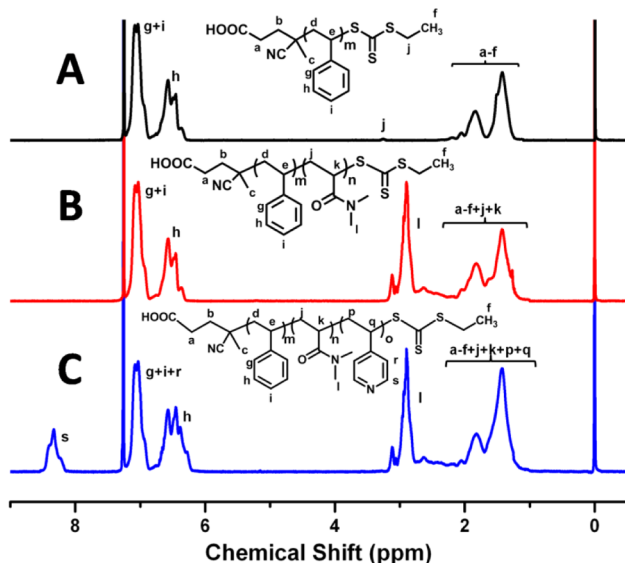


Figure 2.  $^1\text{H}$  NMR spectra of PS<sub>201</sub>-TTC (A), PS<sub>201</sub>-b-PDMA<sub>80</sub>-TTC (B), and the typical PS<sub>201</sub>-b-PDMA<sub>80</sub>-b-P4VP<sub>120</sub> triblock terpolymer (C).

TTC is shown in Figure 2A. Based on the characteristic chemical shift at  $\delta = 7.22\text{--}6.26 \text{ ppm}$  ascribed to the phenyl group in the backbone of PS-TTC and the chemical shift at  $\delta = 3.25 \text{ ppm}$  corresponding to the terminal group originated from the RAFT agent of ECT, the polymer molecular weight  $M_{n,\text{NMR}}$  of the synthesized PS-TTC at 22.8 kg/mol corresponding to DP = 216 is calculated, which is slightly higher than  $M_{n,\text{th}}$  and  $M_{n,\text{GPC}}$  by GPC analysis. In the subsequent discussion, the synthesized PS-TTC is labeled as PS<sub>201</sub>-TTC, in which the DP of 201 is calculated through the theoretical number-average molecular weight  $M_{n,\text{th}}$ .

$$M_{n,\text{th}} = \frac{[\text{monomer}]_0 \times M_{\text{monomer}}}{[\text{RAFT}]_0} \times \text{conversion} + M_{\text{RAFT}} \quad (2)$$

The PS<sub>201</sub>-TTC macro-RAFT agent mediated polymerization of DMA under  $[\text{DMA}]_0:[\text{PS}_{201}\text{-TTC}]_0:[\text{AIBN}]_0 = 300:3:1$  at 79.8% monomer conversion in 2 h led to the targeted PS-b-PDMA-TTC diblock copolymer. Figure 1 shows the GPC traces of the synthesized PS-b-PDMA-TTC diblock copolymer, from which the monomodal GPC traces and the increasing molecular weight compared with the PS<sub>201</sub>-TTC macro-RAFT agent are observed. The molecular weight  $M_{n,\text{GPC}}$  of PS-b-PDMA-TTC by GPC analysis is 25.9 kg/mol (PDI = 1.06), which is smaller than the theoretical molecular weight  $M_{n,\text{th}} = 29.1 \text{ kg/mol}$ . The reason is possibly due to the polystyrene standard employed in the GPC analysis. The  $^1\text{H}$  NMR spectrum of the PS-b-PDMA diblock copolymer is shown in Figure 2B, from which the characteristic chemical shifts due to the protons in the PDMA block are clearly observed. Based on the characteristic chemical shift of the PDMA block at  $\delta = 2.90 \text{ ppm}$  and that in the phenyl groups of the PS block at  $\delta = 7.22\text{--}6.26 \text{ ppm}$ , the  $M_{n,\text{NMR}}$  at 31.0 kg/mol of the PS-b-PDMA diblock copolymer is calculated, which is slightly larger than the  $M_{n,\text{th}}$  calculated by the monomer conversion. This diblock copolymer is labeled as PS<sub>201</sub>-b-PDMA<sub>80</sub>-TTC, in which the subscripts represent the DP of the corresponding blocks calculated by the monomer conversion.

**3.2. Preparation of the PS-b-PDMA-TTC Seed Nanoparticles.** The seed nanoparticles of the PS<sub>201</sub>-b-PDMA<sub>80</sub>-TTC diblock copolymer were prepared similarly with those introduced in our previous work,<sup>58</sup> except that the 8.9 wt % 4VP monomer was added in the present study. The 6.1 wt % dispersion of the PS<sub>201</sub>-b-PDMA<sub>80</sub>-TTC seed nanoparticles as shown in Figure 3A can be prepared by dispersing the PS<sub>201</sub>-b-

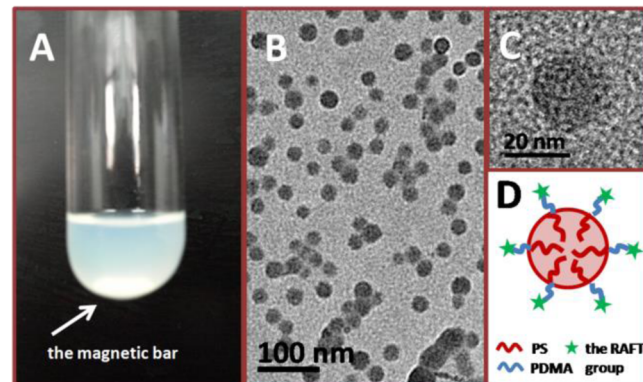
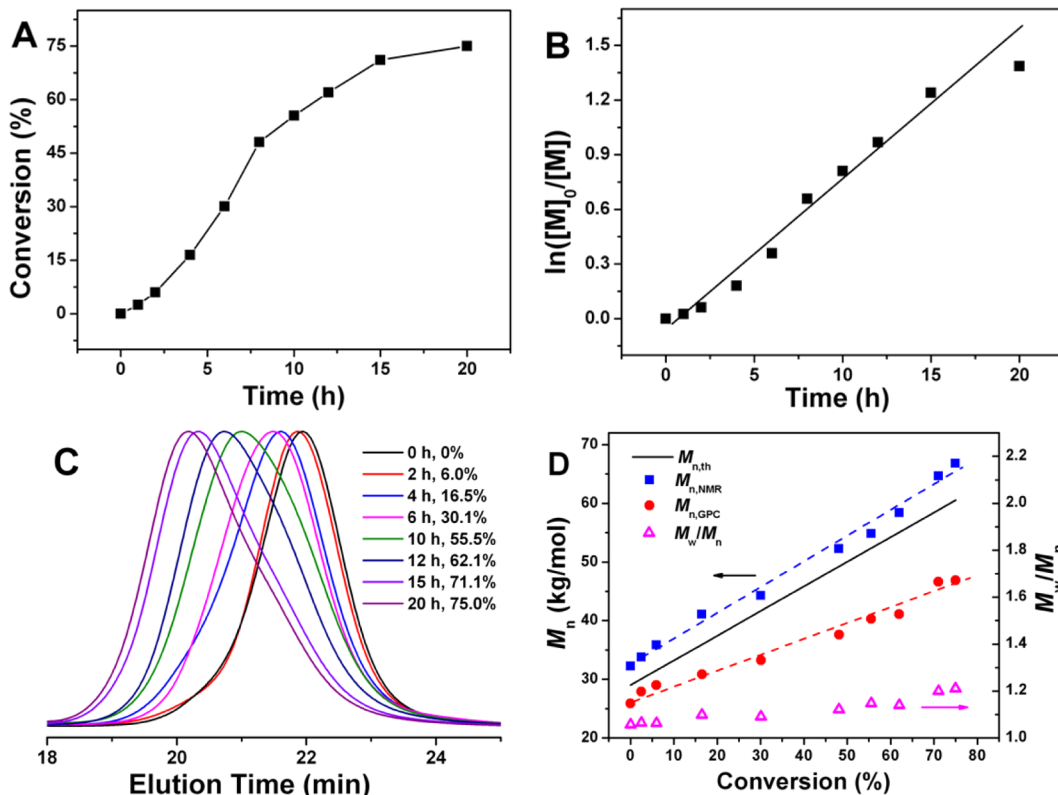
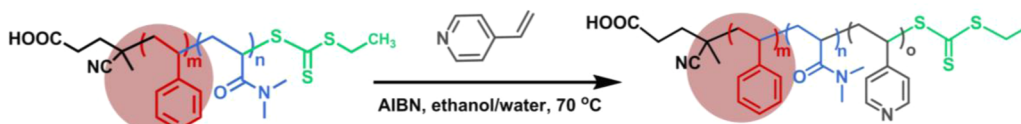


Figure 3. Dispersion of the 6.1 wt % PS<sub>201</sub>-b-PDMA<sub>80</sub>-TTC seed nanoparticles in the ethanol/water/4VP ternary mixture (50/50/10.4 by weight) (A) and the TEM images (B, C) and the schematic structure (D) of the PS<sub>201</sub>-b-PDMA<sub>80</sub>-TTC seed nanoparticles.

PDMA<sub>80</sub>-TTC diblock copolymer in the ternary mixture of ethanol/water/4VP (50/50/10.4 by weight). The TEM images shown in Figures 3B,C suggest that the particle diameter of the seed nanoparticles with the average value at 25 nm is narrowly distributed, which is essential to prepare the BAC triblock copolymer with narrowly distributed molecular weight and low PDI. The DLS analysis also confirmed the narrow size distribution of the PS<sub>201</sub>-b-PDMA<sub>80</sub>-TTC seed nanoparticles with the apparent hydrodynamic diameter ( $D_h$ ) centered at 50

**Scheme 3.** Seeded RAFT Polymerization of 4-Vinylpyridine To Synthesize the PS-*b*-PDMA-*b*-P4VP Triblock Terpolymer Nanoparticles



**Figure 4.** Monomer conversion–time plot (A) and the  $\ln([M]_0/[M])$ –time plot (B) for the seeded RAFT polymerization of 4VP in the presence of the  $\text{PS}_{201}\text{-}b\text{-}\text{PDMA}_{80}\text{-TTC}$  seed nanoparticles, the GPC traces (C), and the molecular weight and PDI (D) of the synthesized  $\text{PS}\text{-}b\text{-}\text{PDMA}\text{-}b\text{-}\text{P4VP}$  triblock terpolymers. Polymerization conditions: 4VP (1.00 g, 9.52 mmol), the ethanol/water mixture (9.60 g, 50/50 by weight),  $[4\text{VP}]_0/[S_{201}\text{-}b\text{-}\text{PDMA}_{80}\text{-TTC}]_0/[AIBN]_0 = 1200/3/1$ ,  $70^\circ\text{C}$ .

nm. The  $\text{PS}_{201}\text{-}b\text{-}\text{PDMA}_{80}\text{-TTC}$  seed nanoparticles are expected to contain a solvophobic PS core and a solvophilic PDMA corona as shown in Figure 3D due to the PS block being insoluble and the PDMA block being soluble in the ethanol/water/4VP ternary mixture. Based on the structure of the  $\text{PS}_{201}\text{-}b\text{-}\text{PDMA}_{80}\text{-TTC}$  diblock copolymer, the Z-group RAFT terminal is located on the outside of the PDMA block as shown in Figure 3D, and therefore the soluble chains of the P4VP block further extend on the outside of the PDMA block to prepare  $\text{PS}\text{-}b\text{-}\text{PDMA}\text{-}b\text{-}\text{P4VP}$  triblock terpolymer nano-objects during the seeded RAFT polymerization.

**3.3. Seeded RAFT Polymerization and in-Situ Synthesis of the Multicompartment Triblock Terpolymer Nanoparticles.** The seeded RAFT polymerization of 4VP was carried out in the 50/50 ethanol/water mixture under  $[4\text{VP}]_0 : [\text{PS}_{201}\text{-}b\text{-}\text{PDMA}_{80}\text{-TTC}]_0 : [AIBN]_0 = 1200:3:1$ . In the 50/50 ethanol/water mixture, both the fed monomer of 4VP and the newly formed third block of P4VP are soluble, and therefore the present seeded RAFT polymerization undergoes somewhat similarly with the homogeneous RAFT polymerization, although the heterogeneous colloidal dispersion is clearly observed by the naked eye. With the progress of the seeded

RAFT polymerization, the third C block of P4VP extends under homogeneous condition (or quasi-homogeneous condition) as shown in Scheme 3, and the diblock copolymer core–corona seed nanoparticles containing a PDMA corona converts into triblock terpolymer core–corona nanoparticles containing a diblock PDMA-*b*-P4VP corona. This polymerization medium of the 50/50 ethanol/water mixture, which is the selective solvent for the C block of P4VP, is chosen to avoid the newly formed P4VP block being entrapped into the PS core of the seed nanoparticles and therefore to form the well-phase-separated core of multicompartment triblock terpolymer nanoparticles. It is expected that, when the polymerization is not performed in the 50/50 ethanol/water mixture but in a nonsolvent for the P4VP block, this entrapment of the newly formed P4VP block in the PS core will somewhat occur, especially when the chain length of the newly formed P4VP block is short in the initial polymerization stage.

The kinetics of the seeded RAFT polymerization are summarized in Figures 4A,B. The monomer conversion increases with the polymerization time and finally reached 75.0% in 20 h, as shown in Figure 4A. The further increase in the polymerization time just leads to a very slight increase in

the monomer conversion. From the linear  $\ln([M]_0/[M])$ –time plot shown in Figure 4B, the pseudo-first-order kinetics of the seeded RAFT polymerization just like a general homogeneous RAFT polymerization is concluded.<sup>61</sup> Figure 4C shows the GPC traces of the PS-*b*-PDMA-*b*-P4VP triblock terpolymers synthesized at different polymerization time (or monomer conversion), from which the molecular weight  $M_{n,\text{GPC}}$  and PDI of the triblock terpolymer are obtained. It is found that the molecular weight  $M_{n,\text{GPC}}$  of the triblock terpolymer increases linearly with the monomer conversion, and  $M_{n,\text{GPC}}$  is slightly lower than the theoretical molecular weight  $M_{n,\text{th}}$  calculated by the monomer conversion (Figure 4D). The PDI values of the PS-*b*-PDMA-*b*-P4VP triblock terpolymers slightly increase with the chains extension of the P4VP block and all the PDI values of the triblock terpolymers are below 1.2. These PS-*b*-PDMA-*b*-P4VP triblock terpolymers are also characterized by <sup>1</sup>H NMR analysis, and the typical <sup>1</sup>H NMR spectra are shown in Figure 2C, from which the molecular weight  $M_{n,\text{NMR}}$  of the triblock terpolymers are calculated by comparing the area ratio of the characteristic chemical shift of the pyridine ring in the P4VP block to that of the benzene ring following eq S1 (see Supporting Information). It is found that  $M_{n,\text{NMR}}$  is close to  $M_{n,\text{th}}$  but is slightly higher than  $M_{n,\text{GPC}}$  by GPC analysis. These results confirm the good control in the molecular weight and weight distribution of the synthesized PS-*b*-PDMA-*b*-P4VP triblock terpolymer in the present seeded RAFT polymerization.

The typical PS<sub>201</sub>-*b*-PDMA<sub>80</sub>-*b*-P4VP<sub>222</sub> triblock terpolymer as well as the reference homopolymer of PS<sub>201</sub>-TTC, PDMA<sub>100</sub>-TTC (see the synthesis in Supporting Information), and P4VP<sub>40</sub> (see the synthesis in ref 62) and the PS<sub>201</sub>-*b*-PDMA<sub>80</sub>-TTC diblock copolymer are further characterized by DSC analysis. As shown in Figure 5, the glass transition temperature

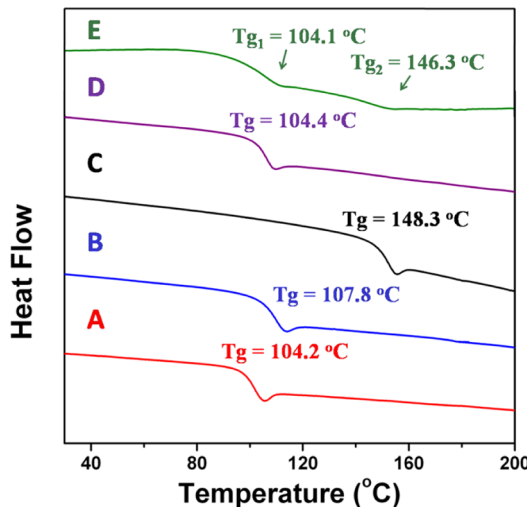


**Figure 5.** DSC thermograms of the homopolymers of PS<sub>201</sub>-TTC (A), PDMA<sub>100</sub>-TTC (B), P4VP<sub>40</sub> (C), the diblock copolymer of PS<sub>201</sub>-*b*-PDMA<sub>80</sub>-TTC (D), and the PS<sub>201</sub>-*b*-PDMA<sub>80</sub>-*b*-P4VP<sub>222</sub> triblock terpolymer (E).

( $T_g$ ) of the reference homopolymers of PS<sub>201</sub>-TTC, PDMA<sub>100</sub>-TTC, and P4VP<sub>40</sub> is 104.2, 107.8, and 148.3 °C, respectively. As to the PS<sub>201</sub>-*b*-PDMA<sub>80</sub>-TTC diblock copolymer, the single  $T_g$  at 104.4 °C is detected, and the reason is possibly due to the two  $T_g$  values of the PS and PDMA blocks being very similar to each other or the PS and PDMA blocks being somewhat

compatible. In the DSC thermograms of the PS<sub>201</sub>-*b*-PDMA<sub>80</sub>-*b*-P4VP<sub>222</sub> triblock terpolymer, two separate  $T_g$  values at 104.1 °C corresponding to the PS and/or PDMA blocks and at 146.3 °C corresponding to the P4VP block are clearly discerned, suggesting the third C block of P4VP is immiscible with the PS block. This immiscible P4VP block with the PS core affords the possibility of in-situ synthesis of the PS-*b*-PDMA-*b*-P4VP multicompartiment nanoparticles as discussed subsequently.

The in-situ synthesized nano-objects of the PS-*b*-PDMA-*b*-P4VP triblock terpolymer were checked by DLS analysis. The polymerization mixture containing the in-situ synthesized triblock terpolymer nano-objects was diluted with the 50/50 ethanol/water mixture, which is just the solvent employed in the seeded RAFT polymerization, and then DLS analysis was made. Figure 6 shows the hydrodynamic diameter ( $D_h$ )

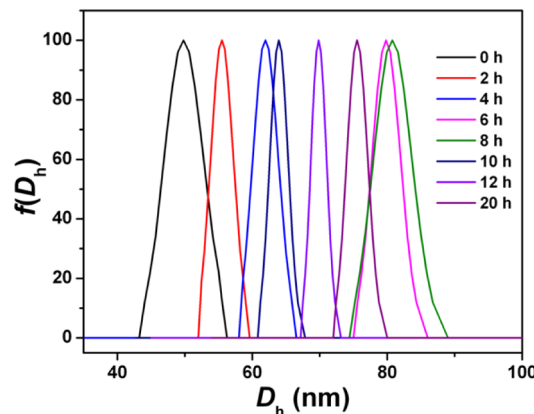


**Figure 6.** Hydrodynamic diameter ( $D_h$ ) distribution of the PS<sub>201</sub>-*b*-PDMA<sub>80</sub>-TTC seed-nanoparticles (0 h) and the PS-*b*-PDMA-*b*-P4VP triblock terpolymer nanoparticles prepared at different polymerization time.

distribution of the PS-*b*-PDMA-*b*-P4VP triblock terpolymer nano-objects with different DP of the newly formed P4VP block prepared at different polymerization time as well as the seed nanoparticles of PS<sub>201</sub>-*b*-PDMA<sub>80</sub>-TTC, in which the narrow  $D_h$  distribution of all the triblock terpolymer nano-objects is concluded. The  $D_h$  of the seed nanoparticles of PS-*b*-PDMA-TTC diblock copolymer is 50 nm, and the  $D_h$  of the PS-*b*-PDMA-*b*-P4VP triblock terpolymer nano-objects gradually increases to 81 nm when the DP of the newly formed P4VP reaches 192. Interestingly, with the further increase in the DP of the newly formed P4VP block, an initial slight decrease and a subsequent slight increase in  $D_h$  as shown in Figure 7 are discerned. Note: the apparent hydrodynamic diameter  $D_h^{\text{app}}$  determined by intensity is afforded herein, and it should be slightly smaller than those by extrapolating  $q^2$  to 0 as discussed elsewhere.<sup>63</sup> This size evolution of the triblock terpolymer nano-objects in the present seeded RAFT polymerization is much different from the seeded dispersion RAFT polymerization<sup>58</sup> and the soluble macro-RAFT agent mediated dispersion polymerization,<sup>64–67</sup> in which the increasing size of the in-situ synthesized block copolymer nano-objects with the extension of the newly formed solvophobic block was detected. The reason for the special size evolution of the triblock terpolymer nano-objects in the present seeded RAFT polymerization is discussed. As known, amphiphilic block copolymers form micelles in the block-selective solvent, and the size or the aggregation number of the amphiphilic block

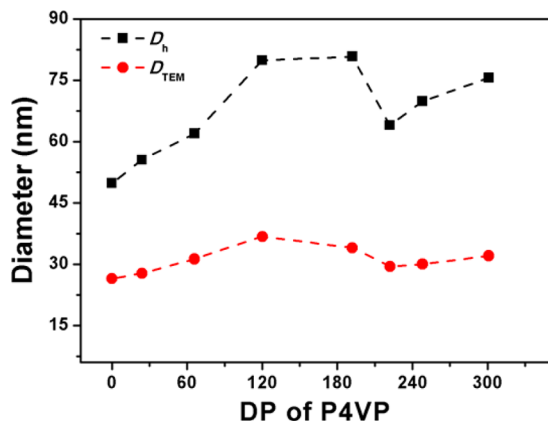


**Figure 7.** Evolution of the average  $D_h$  by DLS analysis and the average diameter  $D_{TEM}$  by TEM observation of the PS-*b*-PDMA-*b*-P4VP nano-objects with the different DP of the P4VP block.

copolymer micelles generally decreases with the DP of the solvophilic block due to the increasing inherent molecular curvature.<sup>68,69</sup> In the present seeded RAFT polymerization, with the monomer conversion, the DP of the newly formed solvophilic P4VP block extends. This DP-increasing P4VP block leads to both positive and negative effects on the size of the PS-*b*-PDMA-*b*-P4VP triblock terpolymer nano-objects. That is, the increase in the DP of the P4VP block leads to the increasing  $D_h$  of the triblock terpolymer nano-objects, if the triblock terpolymer nano-objects are dynamically frozen in the polymerization medium. On the other side, the increase in the DP of the P4VP block enhances the solvophilic character of the triblock terpolymer and leads to the disassociation/reassembly of the triblock terpolymer nano-objects to form size-decreased triblock terpolymer nano-objects as discussed elsewhere.<sup>66</sup> In

the initial stage of the seeded RAFT polymerization, the positive effect is the dominator, and therefore the  $D_h$  of the triblock terpolymer nano-objects increases with the DP of P4VP as shown in Figure 7. In the later stage of the seeded RAFT polymerization, with the extension of the P4VP block, the triblock terpolymer nano-objects become unfrozen in the polymerization medium at the relatively high polymerization temperature, and the size of the triblock terpolymer nano-objects is determined by both the positive and negative effects, and therefore the special size evolution of the triblock terpolymer nano-objects takes place.

To prepare multicompartiment nanoparticles, the in-situ synthesized PS-*b*-PDMA-*b*-P4VP triblock terpolymer nano-objects dispersed in the 50/50 ethanol/water mixture are transferred into water by removing ethanol through N<sub>2</sub> bubbling. Note: P4VP, for example, P4VP<sub>40</sub> ( $M_w = 4200$  Da and PDI = 1.24; see ref 61), is insoluble in neat water and is insoluble in the 10/90 ethanol/water mixture at room temperature even at much diluted 0.01 wt % polymer concentration, and when the ethanol fraction in the ethanol/water mixture is above 25 wt %, P4VP becomes soluble. Clearly, the N<sub>2</sub> bubbling cannot remove all the ethanol in the solvent, and somewhat ethanol (below 5%) remains in the solvent. Despite this, the residual ethanol can be preferentially vaporized during the TEM sampling,<sup>11</sup> and therefore its effect on the soluble-to-insoluble phase transition of the P4VP block to deposit onto the PS core to form PS-*b*-PDMA-*b*-P4VP multicompartiment nanoparticles can be ignored. Besides, to clearly discern the P4VP domain in the PS-*b*-PDMA-*b*-P4VP multicompartiment nanoparticles by TEM observation, the samples are stained by I<sub>2</sub> vapor as discussed elsewhere.<sup>70</sup> Figure 8 shows the TEM images of the PS-*b*-PDMA-*b*-P4VP triblock terpolymer nano-objects synthesized by the seeded RAFT

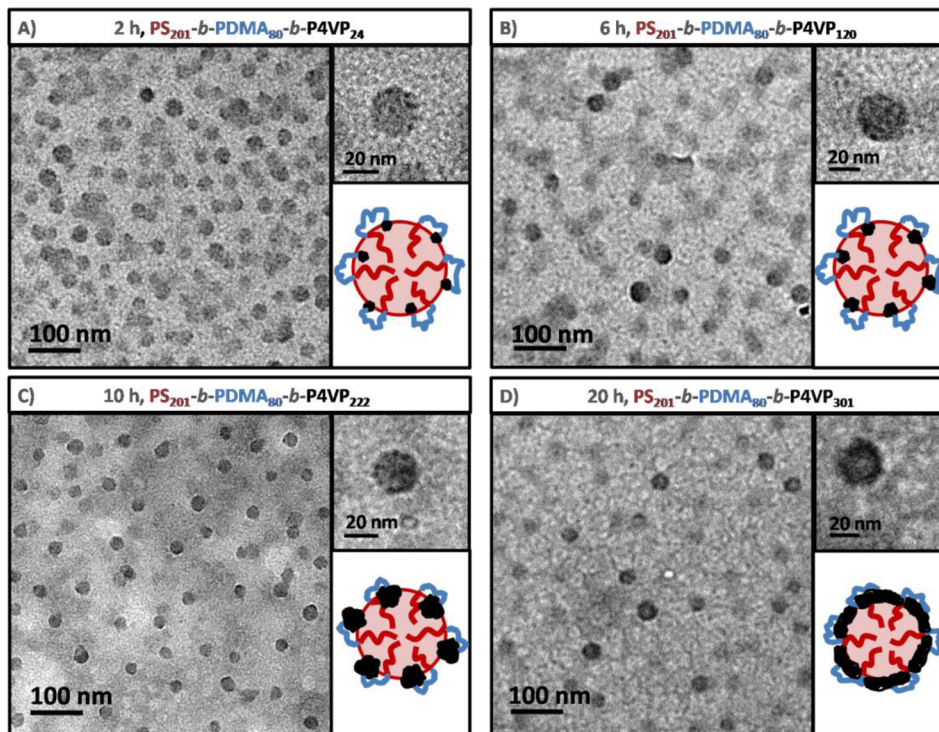
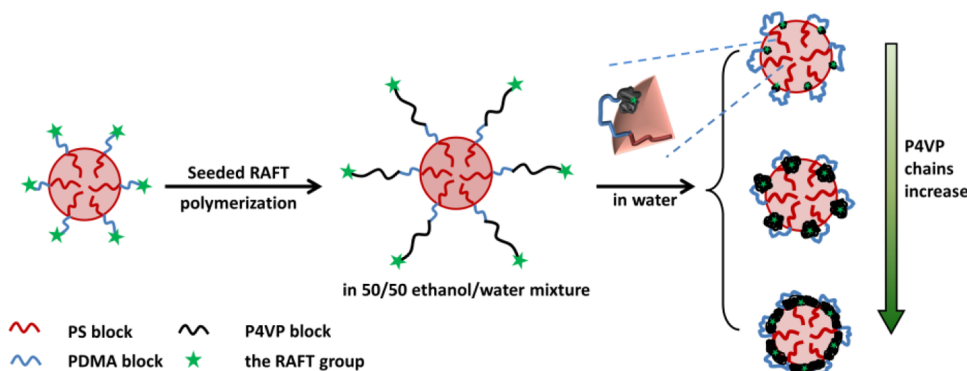


**Figure 8.** Representative TEM images and the schematic structure of the PS-*b*-PDMA-*b*-P4VP multicompartiment nanoparticles prepared at the polymerization time of 2 (A), 6 (B), 10 (C), and 20 h (D).

**Scheme 4.** Schematic in-Situ Synthesis of the PS-*b*-PDMA-*b*-P4VP Multicompartment Nanoparticles by Seeded RAFT Polymerization



polymerization at different polymerization times, in which uniform nanoparticles are observed. By statistical analysis of above 100 nanoparticles, the average diameter  $D_{\text{TEM}}$  of the triblock terpolymer nano-objects is obtained, and the average value is summarized in Figure 7, from which the evolution of  $D_{\text{TEM}}$  with the increasing DP of the newly formed P4VP block similarly with that of  $D_h$  is found. From the high-resolution TEM images, multicompartment nanoparticles with the separated P4VP nodules on the PS core are clearly discerned (Figures 8A–C). Note: the light gray region is the solvophobic PS core, the dark domain is the  $I_2$ -stained P4VP phase deposited on the PS core, and the solvophilic corona of the looped PDMA block is not visible in the TEM images. Based on the high-resolution TEM images, the structure of these multicompartment nanoparticles is schematically shown in Figure 8, in which the B block of PS forms the core, the C block of P4VP forms the nodules, and the A block of PDMA forms the looped corona. Interestingly, with the increase in the DP of the P4VP block from 24 to 222, the P4VP nodules become optically clearer and clearer. The size of the P4VP nodules is estimated to be 2–5 nm, although the size estimation is very approximate. It is expected that the size of the P4VP nodules increases with the DP of the P4VP block. When the DP of the P4VP block further increases to 301, the discrete P4VP nodules transfer into a consecutive P4VP shell to form the concentric core–shell–corona nanoparticles, in which the PS block forms the core, the P4VP block forms the shell, and the looped PDMA block forms the corona as shown in Figure 8.

It is expected that two reasons are ascribed to the successful synthesis of the multicompartment nanoparticles of the linear PS-*b*-PDMA-*b*-P4VP triblock terpolymer. First, the P4VP block is immiscible with the PS block, which leads to the discrete P4VP nodules on the PS core. Second, the present synthesis strategy of the seeded RAFT polymerization avoids the newly formed P4VP block being entrapped in the PS core to form the well-phase-separated core of the triblock terpolymer multicompartment nanoparticles. Compared with the general micellization strategy,<sup>9–22</sup> the present in-situ synthesis strategy affords the convenient preparation of relatively concentrated and well-defined linear triblock terpolymer multicompartment nanoparticles, and the removal of ethanol in the 50/50 ethanol/water mixture by  $N_2$  bubbling depresses the formation of bridged nanoparticles when the P4VP chains deposit on the PS core. Note: the present strategy might not satisfy a strict definition of in-situ synthesis, since an additional and simple procedure of the solvent replace is involved.

Summarily, our main finding is summarized in Scheme 4. Following a so-called seeded RAFT polymerization, concentrated and well-defined BAC triblock terpolymer core–corona nanoparticles of PS-*b*-PDMA-*b*-P4VP containing a solvophobic PS core of the B block and a diblock corona of PDMA (A block) and P4VP (C block) are prepared in the 50/50 ethanol/water mixture, which is the block-selective solvent for the PDMA and P4VP blocks but the nonsolvent for the PS block. By transferring the BAC triblock terpolymer nanoparticles into water, the P4VP block becomes insoluble and deposits on the PS core to form discrete P4VP nodules and therefore leads to multicompartment nanoparticles. With the increase in the DP of the P4VP block, the multicompartment nanoparticles containing discrete P4VP nodules converts into concentric core–shell–corona nanoparticles, in which the PS block forms the core, the P4VP block forms the shell, and the looped PDMA block forms the corona.

#### 4. CONCLUSIONS

A new strategy of in-situ synthesis (or quasi-in-situ synthesis) of multicompartment nanoparticles of the linear BAC triblock terpolymer of PS-*b*-PDMA-*b*-P4VP is proposed. Following this strategy, the seeded RAFT polymerization of 4VP in the 50/50 ethanol/water mixture, which is the solvent for the C block of the newly formed P4VP block, is performed in the presence of the PS-*b*-PDMA-TTC seed nanoparticles with the Z-group RAFT terminal at the outer side of the A block of the PDMA block, and well-defined core–corona nanoparticles of PS-*b*-PDMA-*b*-P4VP containing PS core and a diblock corona of PDMA-*b*-P4VP dispersed in the 50/50 ethanol/water mixture are formed. When the triblock terpolymer nanoparticles are transferred into water, which is the nonsolvent for the newly formed P4VP block and whereas is a solvent for the central PDMA block, the P4VP block deposits on the PS core to form discrete P4VP nodules to form the PS-*b*-PDMA-*b*-P4VP multicompartment nanoparticles. The linear BAC triblock terpolymer multicompartment nanoparticles are composed of a PS core, nodules of the P4VP block, and a looped PDMA corona. With the increasing DP of the P4VP block, multicompartment nanoparticles can convert into concentric core–shell–corona nanoparticles, in which the PS block forms the core, the P4VP block forms the shell, and the looped PDMA block forms the corona. The present strategy has the advantage of convenient preparation of relatively concentrated and well-defined linear triblock terpolymer multicompartment nanoparticles or concentric core–shell–corona nanoparticles. Two

reasons including the (1) the P4VP block being immiscible with the PS block and (2) the special seeded RAFT polymerization are ascribed to the successful preparation of the linear triblock terpolymer multicompartiment nanoparticles.

## ASSOCIATED CONTENT

### Supporting Information

Equation S1 showing the calculation of the  $M_{n,NMR}$  of the synthesized PS-*b*-PDMA-*b*-P4VP triblock terpolymers and the text showing the synthesis and characterization of PDMA<sub>100</sub>-TTC. This material is available free of charge via the Internet at <http://pubs.acs.org>.

## AUTHOR INFORMATION

### Corresponding Author

\*E-mail: wqzhang@nankai.edu.cn, Tel 86-22-23509794, Fax 86-22-23503510 (W.Z.).

### Notes

The authors declare no competing financial interest.

## ACKNOWLEDGMENTS

The financial support by National Science Foundation of China (No. 20974051 and 21074059), NFFTBS (No. J1103306) and PCSIRT (IRT1257) is gratefully acknowledged.

## REFERENCES

- (1) Laschewsky, A. *Curr. Opin. Colloid Interface Sci.* **2003**, *8*, 274–281.
- (2) Lutz, J.-F.; Laschewsky, A. *Macromol. Chem. Phys.* **2005**, *206*, 813–817.
- (3) Amado, E.; Kressler, J. *Soft Matter* **2011**, *7*, 7144–7149.
- (4) Moughton, A. O.; Hillmyer, M. A.; Lodge, T. P. *Macromolecules* **2012**, *45*, 2–19.
- (5) Ringsdorf, H.; Lehmann, P.; Weberskirch, R. Multicompartment – a concept for the molecular architecture of life. In 217th ACS National Meeting, Anaheim, CA, 1999.
- (6) Du, J.; Reilly, R. K. *Chem. Soc. Rev.* **2011**, *40*, 2402–2416.
- (7) Jiang, T.; Wang, L.; Lin, S.; Lin, J.; Li, Y. *Langmuir* **2011**, *27*, 6440–6448.
- (8) Wang, L.; Lin, J. *Soft Matter* **2011**, *7*, 3383–3391.
- (9) Kubowicz, S.; Baussard, J.-F.; Lutz, J.-F.; Thünemann, A. F.; Berlepsch, H. v.; Laschewsky, A. *Angew. Chem., Int. Ed.* **2005**, *44*, 5262–5265.
- (10) Skrabania, K.; Berlepsch, H. v.; Böttcher, C.; Laschewsky, A. *Macromolecules* **2010**, *43*, 271–281.
- (11) Skrabania, K.; Laschewsky, A.; Berlepsch, H. v.; Böttcher, C. *Langmuir* **2009**, *25*, 7594–7601.
- (12) Marsat, J.-N.; Heydenreich, M.; Kleinpeter, E.; Berlepsch, H. v.; Böttcher, C.; Laschewsky, A. *Macromolecules* **2011**, *44*, 2092–2105.
- (13) Ott, C.; Hoogenboom, R.; Hoeppener, S.; Wouters, D.; Gohy, H.-F.; Schubert, U. S. *Soft Matter* **2009**, *5*, 84–91.
- (14) Gao, Y.; Li, X.; Hong, L.; Liu, G. *Macromolecules* **2012**, *45*, 1321–1330.
- (15) Kyeremateng, S. O.; Busse, K.; Kohlbrecher, J.; Kressler, J. *Macromolecules* **2011**, *44*, 583–593.
- (16) Weberskirch, R.; Preuschen, J.; Spiess, H. W.; Nuyken, O. *Macromol. Chem. Phys.* **2000**, *201*, 995–1007.
- (17) Gröschel, A. H.; Walther, A.; Löbling, T. I.; Schmelz, J.; Hanisch, A.; Schmalz, H.; Müller, A. H. E. *J. Am. Chem. Soc.* **2012**, *134*, 13850–13860.
- (18) Zhou, C.; Hillmyer, M. A.; Lodge, T. P. *J. Am. Chem. Soc.* **2012**, *134*, 10365–10368.
- (19) Dupont, J.; Liu, G. *Soft Matter* **2010**, *6*, 3654–3661.
- (20) Uchman, M.; Štěpánek, M.; Procházka, K. *Macromolecules* **2009**, *42*, 5605–5613.
- (21) Cao, Y.; Zhao, N.; Wu, K.; Zhu, X. X. *Langmuir* **2008**, *25*, 1699–1704.
- (22) Sugihara, S.; Kanaoka, S.; Aoshima, S. *J. Polym. Sci., Part A: Polym. Chem.* **2004**, *42*, 2601–2611.
- (23) Gohy, J.-F.; Ott, C.; Hoeppener, S.; Schubert, U. S. *Chem. Commun.* **2009**, *9*, 6038–6040.
- (24) Tsitsilianis, C.; Stavrouli, N.; Bocharova, V.; Angelopoulos, S.; Kiriy, A.; Katsampas, I.; Stamm, M. *Polymer* **2008**, *49*, 2996–3006.
- (25) Hsu, Y.-C.; Huang, C.-I.; Li, W.; Qiu, F.; Shi, A.-C. *Polymer* **2013**, *54*, 431–439.
- (26) Shunmugam, R.; Smith, C. E.; Tew, G. N. *J. Polym. Sci., Part A: Polym. Chem.* **2007**, *45*, 2601–2608.
- (27) Taribagil, R. R.; Hillmyer, M. A.; Lodge, T. P. *Macromolecules* **2010**, *43*, 5396–5404.
- (28) Li, Z.; Kesselman, E.; Talmon, Y.; Hillmyer, M. A.; Lodge, T. P. *Science* **2004**, *306*, 98–101.
- (29) Li, Z.; Hillmyer, M. A.; Lodge, T. P. *Langmuir* **2006**, *22*, 9409–9417.
- (30) Saito, N.; Liu, C.; Lodge, T. P.; Hillmyer, M. A. *Macromolecules* **2008**, *41*, 8815–8822.
- (31) Walther, A.; Müller, A. H. E. *Chem. Commun.* **2009**, *9*, 1127–1129.
- (32) Hanisch, A.; Gröschel, A. H.; Förtsch, M.; Drechsler, M.; Jinmai, H.; Ruhland, T. M.; Schacher, F. H.; Müller, A. H. E. *ACS Nano* **2013**, *7*, 4030–4041.
- (33) Ge, Z.; Liu, S. *Macromol. Rapid Commun.* **2009**, *30*, 1523–1532.
- (34) Mao, J.; Ni, P.; Mai, Y.; Yan, D. *Langmuir* **2007**, *23*, 5127–5134.
- (35) Pochan, D. J.; Zhu, J.; Zhang, K.; Wooley, K. L.; Miesch, C.; Emrick, T. *Soft Matter* **2011**, *7*, 2500–2506.
- (36) Zhu, J.; Zhang, S.; Zhang, K.; Wang, X.; Mays, J. W.; Wooley, K. L.; Pochan, D. J. *Nat. Commun.* **2013**, *4*, 2297.
- (37) Zhu, J.; Hayward, R. C. *Macromolecules* **2008**, *41*, 7794–7797.
- (38) Liu, X.; Gao, H.; Huang, F.; Pei, X.; An, Y.; Zhang, Z.; Shi, L. *Polymer* **2013**, *54*, 3633–3640.
- (39) Gohy, J.-F.; Lefevre, N.; D'Haese, C.; Hoeppener, S.; Schubert, U. S.; Kostov, G.; Ameduri, B. *Polym. Chem.* **2011**, *2*, 328–332.
- (40) Kotzev, A.; Laschewsky, A.; Adriaensens, P.; Gelan, J. *Macromolecules* **2002**, *35*, 1091–1101.
- (41) Szczubialka, K.; Moczek, L.; Goliszek, A.; Nowakowska, M.; Kotzev, A.; Laschewsky, A. *J. Fluorine Chem.* **2005**, *126*, 1409–1418.
- (42) Babinot, J.; Renard, E.; Droumaguet, B. L.; Guigner, J.-M.; Mura, S.; Nicolas, J.; Couvreur, P.; Langlois, V. *Macromol. Rapid Commun.* **2013**, *34*, 362–368.
- (43) Barthel, M. J.; Mansfeld, U.; Hoeppener, S.; Czaplewski, J. A.; Schacher, F. H.; Schubert, U. S. *Soft Matter* **2013**, *9*, 3509–3520.
- (44) Hu, X.; Tong, Z.; Lyon, L. A. *J. Am. Chem. Soc.* **2010**, *132*, 11470–11472.
- (45) Li, Z.; Ma, J.; Lee, N. S.; Wooley, K. L. *J. Am. Chem. Soc.* **2011**, *133*, 1228–1231.
- (46) Jiang, X.; Zhang, G.; Narain, R.; Liu, S. *Langmuir* **2009**, *25*, 2046–2054.
- (47) Kempe, K.; Hoogenboom, R.; Hoeppener, S.; Fustin, C.-A.; Gohy, J.-F.; Schubert, U. S. *Chem. Commun.* **2010**, *46*, 6455–6457.
- (48) Kim, J.-W.; Suh, K.-D. *J. Ind. Eng. Chem.* **2008**, *14*, 1–9.
- (49) Tang, C.; Zhang, C.; Liu, J.; Qu, X.; Li, J.; Yang, Z. *Macromolecules* **2010**, *43*, 5114–5120.
- (50) Fujibayashi, T.; Okubo, M. *Langmuir* **2007**, *23*, 7958–7962.
- (51) Gonçalves, O. H.; Asua, J. M.; de Araújo, P. H. H.; Machado, R. A. F. *Macromolecules* **2008**, *41*, 6960–6964.
- (52) Zhou, W.; Yu, W.; An, Z. *Polym. Chem.* **2013**, *4*, 1921–1931.
- (53) Chambon, P.; Blanazs, A.; Battaglia, G.; Armes, S. P. *Macromolecules* **2012**, *45*, 5081–5090.
- (54) Chenal, M.; Bouteiller, L.; Rieger, J. *Polym. Chem.* **2013**, *4*, 752–762.
- (55) Ganeva, D. E.; Sprong, E.; de Bruyn, H.; Warr, G. G.; Such, C. H.; Hawkett, B. S. *Macromolecules* **2007**, *40*, 6181–6189.
- (56) Bowes, A.; Mclearay, J. B.; Sanderson, R. D. *J. Polym. Sci., Part A: Polym. Chem.* **2007**, *45*, 588–604.
- (57) Wei, R.; Luo, Y.; Li, Z. *Polymer* **2010**, *51*, 3879–3886.

- (58) Huo, F.; Gao, C.; Dan, M.; Xiao, X.; Su, Y.; Zhang, W. *Polym. Chem.* **2014**, DOI: 10.1039/C3PY01569F.
- (59) Moad, G.; Rizzardo, E.; Thang, S. H. *Aust. J. Chem.* **2006**, *59*, 669–692.
- (60) Allen, M. H., Jr.; Hemp, S. T.; Smith, A. E.; Long, T. E. *Macromolecules* **2012**, *45*, 3699–3676.
- (61) Lowe, A. B.; McCormick, C. L. *Prog. Polym. Sci.* **2007**, *32*, 283–351.
- (62) Zhang, W.; Shi, L.; An, Y.; Wu, K.; Gao, L.; Liu, Z.; Ma, R.; Zhao, C.; He, B. *Macromolecules* **2004**, *37*, 2924–2929.
- (63) Zhang, W.; Shi, L.; Wu, K.; An, Y. *Macromolecules* **2005**, *38*, 5743–5747.
- (64) Charleux, B.; Delaittre, G.; Rieger, J.; D'Agosto, F. *Macromolecules* **2012**, *45*, 6753–6765.
- (65) Sun, J.-T.; Hong, C.-Y.; Pan, C.-Y. *Polym. Chem.* **2013**, *4*, 873–881.
- (66) Semsarilar, M.; Ladmiral, V.; Blanazs, A.; Armes, S. P. *Langmuir* **2012**, *28*, 914–922.
- (67) Su, Y.; Xiao, X.; Li, S.; Dan, M.; Wang, X.; Zhang, W. *Polym. Chem.* **2014**, *5*, 578–587.
- (68) de Graaf, A. J.; Boere, K. W. M.; Kemmink, J.; Fokkink, R. G.; van Nostrum, C. F.; Rijkers, D. T. S.; van der Gucht, J.; Wienk, H.; Baldus, M.; Mastrobattista, E.; Vermonden, T.; Hennink, W. E. *Langmuir* **2011**, *27*, 9843–9848.
- (69) He, Y.; Li, Z.; Simone, P.; Lodge, T. P. *J. Am. Chem. Soc.* **2006**, *128*, 2745–2750.
- (70) Pale, V.; Nikkonen, T.; Vapaavuori, J.; Kostiainen, M.; Kavakka, J.; Selin, J.; Tittonen, I.; Helaja, J. *J. Mater. Chem. C* **2013**, *1*, 2166–2173.